Materials Advances

ROYAL SOCIETY OF CHEMISTRY

REVIEW

View Article Online
View Journal | View Issue

Cite this: *Mater. Adv.*, 2023, 4, 35

Responsive and reactive layer-by-layer coatings for deriving functional interfaces

Dibyangana Parbat*[ad] and Uttam Manna *[abc]

Evolution in biological systems has led to various unique and fascinating properties with astounding complexity guided by mother nature for billions of years. Inspired by nature's design, tailoring functional interfaces with multi-scale hierarchy is of potential interest for current scientific and engineering research owing to their broad range of versatile applications in thriving scientific disciplines like biomedical, surface engineering, nanotechnology, and many more. In comparison to the existing techniques, the layer-by-layer (LbL) deposition method is highly acknowledged for its huge contribution in developing various functional interfaces as this method possesses some extraordinary advantages like versatility, simple preparation procedure, substrate-independent nature, and fine control over both topography and thickness of the coating. The LbL deposited coatings that were either stimuli-responsive or readily and selectively chemically reactive appeared as an emerging approach for deriving various functional interfaces. Here, the progress of stimuli-responsive and chemically reactive multilayer coatings (CRMLCs) has been adequately presented. Thereafter, the various prospective applications of both stimuli-responsive and CRMLCs are introduced in this review.

Received 30th June 2022,
Accepted 22nd September 2022

DOI: 10.1039/d2ma00791f

rsc.li/materials-advances

[a] *Department of Chemistry, Indian Institute of Technology-Guwahati, Kamrup, Assam 781039, India. E-mail: d.parbat22@gmail.com, umanna@iitg.ac.in*
[b] *Centre for Nanotechnology, Indian Institute of Technology-Guwahati, Kamrup, Assam 781039, India*
[c] *School of Health Science & Technology, Indian Institute of Technology-Guwahati, Kamrup, Assam 781039, India*
[d] *Department of Mechanical Engineering, Pohang University of Science and Technology, Pohang, 37673, Korea*

Dibyangana Parbat

Dr Dibyangana Parbat is currently working as Brain-Korea (BK) 21 Post-doctoral fellow at Pohang University of Science and Technology (POSTECH), Korea. She has been working on bio-inspired polymeric interfaces/multilayers and their various applications in various applied contexts. She was awarded IOE-IISc post-doctoral fellowship and SERB-national post-doctoral fellowship in 2021. She received her PhD from IIT, Guwahati, under the guidance of Dr Uttam Manna in 2021. Her research interest involves bio-inspired wettability, surface modification, drag-reduction and polymer synthesis. She has synthesized various bio-mimicked interfaces/multilayers and investigated their performance in removing oil-spillages, controlling platelet adhesion, preparing patterned interfaces, etc. Her research works were selected for several national and international awards.

Uttam Manna

Dr Uttam Manna, an Invited Fellow of the Royal Society of Chemistry (FRSC), currently an associate professor at the Indian Institute of Technology Guwahati, completed his PhD at IISc Bangalore in 2011. He pursued his postdoctoral research at the University of Wisconsin–Madison from 2011–2015. He has been selected as an associate of the Indian Academy of Sciences in 2018. He is a recipient of both the NASI-Young Scientist Platinum Jubilee Award-2018 and INSA-Medal for Young Scientist-2019. Journal of Materials Chemistry A (2018), Chemical Communications (2020) and Nanoscale (2021) recognized him as an emerging investigator. Since early 2021, he has been an advisory board member of Materials Horizons. His research team is involved in designing functional and durable bio-inspired wettability through strategic use of catalyst free and simple chemical reactions under ambient conditions.

1. Introduction

Layer-by-layer (LbL) interfaces decorated with various attractive functionalities have evolved and thrived over time, mostly inspired by nature's patterns.[1–5] For instance, various multilayers have attracted a lot of attention owing to their diverse potential in designing biomimicked interfaces like lotus leaf-inspired superhydrophobic surfaces,[6–8] fish scale-inspired underwater superoleophobic surfaces,[9,10] and nepenthes pitcher plant-inspired[11,12] slippery liquid-infused porous surfaces (SLIPSs),[11–13] which exhibit either extremes of liquid (water/oil) repellency (in air or under water) with an advancing liquid contact angle (CA) of $\geq 150^\circ$ and contact angle hysteresis (CAH) $\leq 10^\circ$ or slippery properties towards various liquid phases in air[12] (Fig. 1). Various naturally existing interfaces, including lotus leaf, butterfly wings,[2] fish scales,[11] nepenthes pitcher, *etc.* (Fig. 1), are inherently associated with the required hierarchical topography and appropriate chemistry on top to display superhydrophobicity, slippery properties, underwater superoleophobicity, *etc.* Hence, the design of an appropriate hierarchical topography that can be modified with adequate chemicals remained instrumental in developing desired bio-inspired wettability. In this context, LbL deposition techniques have been strategically employed to mimic such nature-inspired properties as shown in Fig. 1. Apart from these bio-inspired wettabilities, other different functional interfaces were synthesized using the LbL self-assembly technique. These include, for example, self-healing surfaces with enhanced durability of the material, resulting in long-term stability of the material for practical use,[14] and various biologically relevant interfaces with an ability to control different cell/substrate interactions and related bioactivity,[15,16] as shown in Fig. 1.

The stimuli-induced reversible change in the shape/structure/wettability of LbL interfaces is responsible for actuation behaviour,[17] biosensing applications,[18] *etc.* These interfaces have prospects for application in various practically relevant contexts. Research on such multilayer coatings in tailoring functional interfaces has been growing rapidly in the past few decades.[19–22] This approach provided a common platform for tailoring appropriate topography and desired chemistry. For example, the same hierarchically (micro/nano) featured surface can exhibit

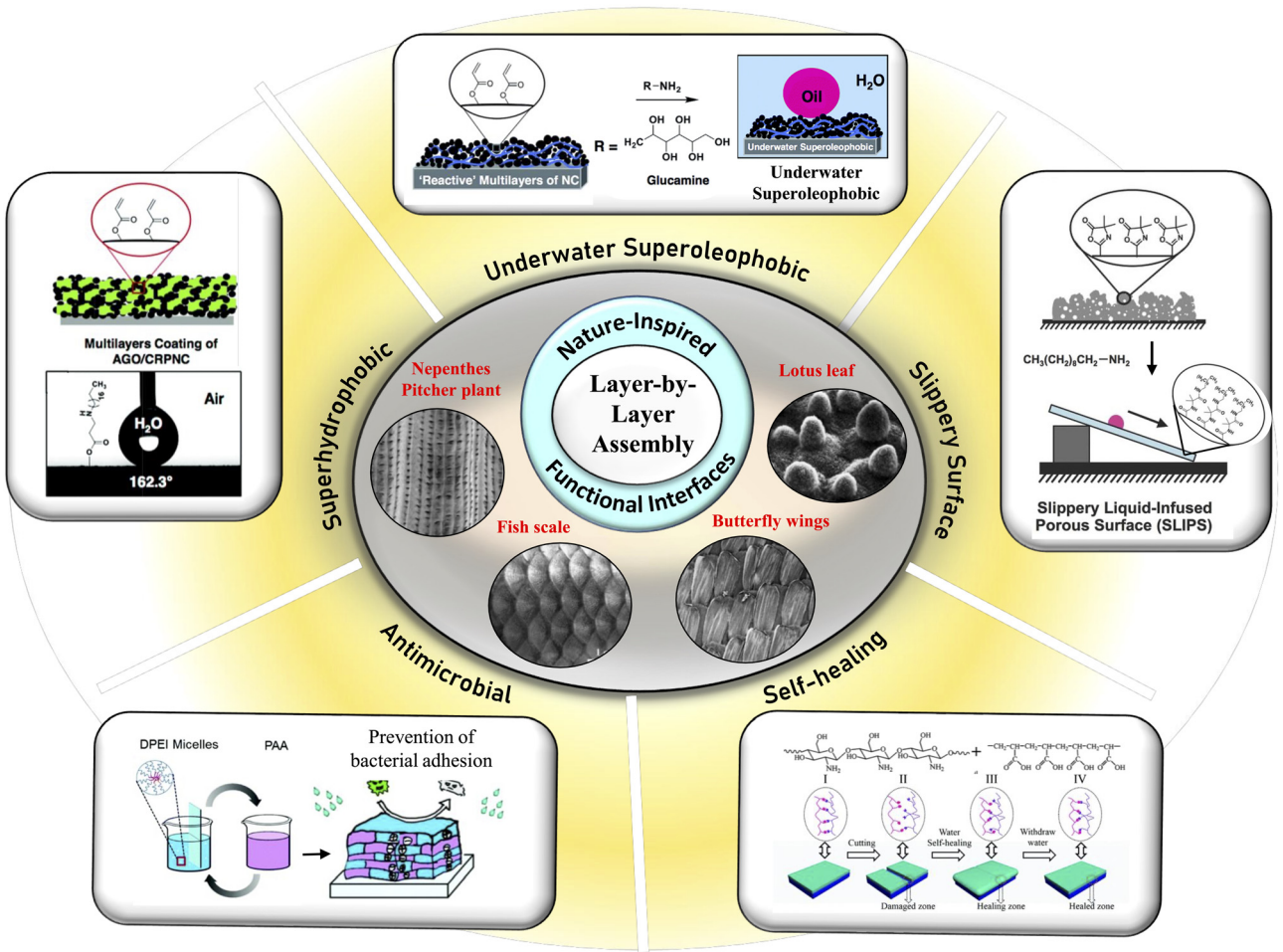

Fig. 1 Morphological architectures (SEM images) of naturally existing functional interfaces like lotus leaf, butterfly wings, fish scale and nepenthes pitcher plant. Inspired by nature, various synthetic interfaces have been fabricated through the LbL deposition method to achieve different bio-inspired wettability, including superhydrophobicity, underwater superoleophobicity, slippery properties, *etc.* Some of the multilayer coatings were also successfully applied to demonstrate self-healing ability and antimicrobial activity. Reprinted with permission from ref. 2, 6, 8–11, 13, 14 and 16.

superhydrophobic properties, underwater superoleophobic properties, or slippery properties depending on the adequate post-chemical modulations.[23] At the same time, such micro/nano-scaled topography with desired cross-linking chemistries is also involved in mimicking the sophisticated cellular environment to achieve a biocompatible interface capable of controlling various cell functions like adhesion, encapsulation, proliferation, *etc.*[15,24] Moreover, a distinct chemical architecture along with chemical interactions, like electrostatic interactions,[25] hydrogen bonds,[26,27] coordination bonds,[28] guest–host interactions,[29] covalent interactions,[30] and the combined interactions of the above-mentioned forces, is often employed to design self-healing materials.[14,31,32] On that basis, it can be inferred that the key components of introducing different functions in various materials are topographical features, and selection of specific chemical components and their spatial arrangements/interactions in the multilayer assembly. Understanding the rudiments of various functional properties is expected to help in explaining the underlying intricacies of these interfaces and various approaches of fabrication.

Plenty of methodologies such as lithographic patterning,[33,34] laser/plasma etching,[35,36] templating,[37,38] sol–gel method,[39–41] chemical vapor deposition,[42,43] electrospinning,[44] spin coating,[45] and so forth[46,47] have been introduced for the fabrication of such functional interfaces with impeccable properties. Although all of these approaches are equipped with several advantages concerning the demand of achieving the essential criteria, most of these methods need expensive instrumentation and involve complex fabrication procedures which appear as a major constraint to the commercial use of such interfaces.[48,49] Therefore, some simple methodologies with cost-effective work regimes are still highly desirable to extend the real-life applications of these functional interfaces.

In the past, the layer-by-layer (LbL) assembly approach achieved enormous attention because of its versatile nature and easy execution for the strategic construction of composite multilayers with controlled precision over topography and selective chemical composition.[50] Various advanced materials have been successfully synthesized by designing the multilayer coating consisting of different components like block copolymers,[51] polymeric microgels,[52] polyelectrolytes,[53,54] biomacromolecules,[55] dendritic polymers,[56] *etc.* Different and relevant interactions are responsible for the construction of LbL multilayer coatings which include electrostatic interactions,[57,58] hydrogen-bonds,[59,60] halogen-bonds,[61] coordination bonds,[62,63] charge-transfer interactions,[64] guest–host interactions,[65] *etc.* Apart from these interactions, recently various covalent bonds have also been explored in developing LbL assembly.[66–68]

Exploring new materials for LbL assembly will be enriching the structures and will widen the scope of functionalities in LbL-fabricated materials. In the past, stimuli-responsive multilayers, consisting of polyelectrolytic/polymeric multilayers, were mostly explored in developing various functional and dynamic interfaces mentioned above using UV, heat, magnetism, pH, *etc.* as external stimuli.[69] While a remarkable breakthrough in the development of such multilayer coatings has been made in the field of biomedical engineering,[70] surface engineering,[71] *etc.*, the impacts of the durability of such interfaces limit their application in practical scenarios. Recently, studies of chemically reactive multilayer coatings (CRMLCs)[72] have guided one to achieve a durable design with tunable reactivity for tailoring interfaces with desired and adequate functionality and promoting their application in diverse prospective areas.[73]

In this review, we intend to give an overview of the recent attempts towards the progress of LbL multilayer coatings in surface engineering to develop multi-functional interfaces and discuss both stimuli-responsive and CRMLCs to achieve and control various functions *via* adopting a facile LbL deposition process. The review starts with a general discussion and overview of various functional interfaces followed by the contribution of the LbL assembly method in fabricating such interfaces. In subsequent sections, we have discussed the systematic advancement of the LbL technique regulating the progression of functional interfaces from the following aspects: (i) different designs of stimuli-responsive and chemically reactive multilayer coatings and (ii) the application of both stimuli-responsive and chemically reactive multilayer coatings in the fabrication of various functional interfaces.

2. Designs of stimuli-responsive and chemically reactive multilayer coatings

The LbL deposition approach[74] is a versatile and simple approach (Fig. 1) for designing functional interfaces by adjusting the morphology as well as chemistry.[50] Moreover, the thickness and architecture of the prepared coating can be controlled strategically even with molecular precision.[50,68,71–73] The construction of electrostatic interaction-driven multilayer assembly is found to be entropy-driven as the counter ions are released in this process.[74] Various advantages, such as (i) an easy and uncomplicated fabrication process, (ii) controlled modulation of multilayer thickness down to the nanometer scale and (iii) a surface-independent nature, make this fabrication method distinct and special from other approaches.[75,76] One major limitation of the LbL technique is its time-consuming deposition process. Typically, the time required to assemble one layer through electrostatic interaction is a few minutes, although the time may vary based on the constituents and associated interactions. To resolve this drawback, attempts are being made to expedite the deposition process and automated devices have also been proposed for scaling up the multilayer coatings.[77–79]

In the past, lots of multilayer coatings that were developed *via* the LbL deposition technique were made of selected and complementary polyelectrolytes.[53–58,70,71] The use of labile electrostatic interaction for constructing the basic architecture of the coating inherently affected the physical and chemical durability of the multilayer assemblies.[80–82] In contrast, various covalently cross-linked 'reactive' chemistries like azlactone–amine reactions, Michael addition reactions, Schiff-base reactions, epoxy ring-opening reactions, thiol–ene click chemistry, *etc.*[83–88] have been utilized for developing functional and durable materials.

While the covalent chemical crosslinking improves both physical and chemical durability of the multilayers, the residual reactivity of the coating towards various chemical functionalities enables the fabrication of various functional multilayer coatings. The design of reactive polymers and their reactive multilayer coatings provide a platform to modify multilayer coatings with selected chemicals to achieve desired properties.[72,89] Various reactive polymers like chitosan, branched poly(ethyleneimine) (BPEI), poly(2-vinyl-4,4-dimethylazlactone) (PVDMA), *etc.* are mostly involved in forming covalent crosslinking between two adjacent layers during the LbL deposition process.[90,91] Further chemical modification is possible because of residual reactive groups of such polymers leading to the development of different functional interfaces. In order to enhance the structural features of coatings and achieve suitable morphology for particular applications, the incorporation of nanoparticles in the multilayer system is often demonstrated in the literature.[92]

In this section, two distinct and important classes of multilayer coatings, *i.e.*, stimuli-responsive and chemically reactive multilayer coatings, are presented in detail. The multilayer coatings which can exhibit responsiveness to various applied stimuli are generally referred to as stimuli-responsive multilayers and such interfaces are important for various smart applications like drug delivery, droplet manipulation, *etc.* On the other hand, chemically reactive multilayers that are loaded with some selectively and readily reactive moieties offer a facile basis to modify their chemistry for various intended applications. These multilayers which are capable of showing dynamic and stimuli-responsive properties are discussed in the following sections in more detail.

2.1. Stimuli-responsive LbL multilayer

In the last few years, a huge interest has been developed in synthesizing advanced multifunctional systems with distinct topography, composition, property, and functions for designing a dynamic smart/intelligent system that is responsive to different external stimuli[93] as shown in Fig. 2. Such systems were mostly and commonly developed through the strategic use of selective stimuli responsive molecules or polymers or nanomaterials.

Multilayer assemblies built by the LbL assembly approach have shown great potential to adapt and respond to desired external conditions, thus leading to novel well-defined smart functional systems to meet the specific requirements of different applications. The responsiveness of LbL multilayer assemblies can enable us to achieve spatial, temporal, and active control over the physicochemical properties by controlling specific internal structure, composition, or triggers (*e.g.*, pH, ionic strength, temperature, magnetic, electric or ultrasonic fields, light, redox potential, mechanical stress, biomolecules or ionic surfactants).[94–96] Stimuli-responsive LbL systems mostly undergo changes in their physicochemical properties (*e.g.*, size, shape, conformation, thickness, solubility, swelling/shrinking behavior, hydrophilic/hydrophobic balance, or release of a bioactive molecule) owing to the interruption of weaker intermolecular interactions between the adsorbed layers through the application of specific external stimuli.[1]

Hu *et al.*[94] reported a triple-responsive LbL film where (i) light was used as one of the external stimuli to delaminate a free-standing film, (ii) a covalently bound dye was released from the free-standing film upon chemical reduction of that film, and (iii) an increase in pH dissolved the film. The film was prepared by first depositing PSS and a photodegradable polycation P1 (prepared from the methylated nitrobenzyl methacrylate monomer and *N*,*N*-dimethylaminoethylmethacrylate (DMAEMA) that has pendants methylated in the benzylic position; Fig. 3A) on a plasma cleaned quartz substrate followed by depositing PSS and redox/pH dual responsive polycation P2 (prepared through random copolymerization of DMAEMA, coumarinyl methacrylate (CMA), and methacrylate with rhodamine linked through a disulfide bond; Fig. 3B). The remaining P2/PSS film could be peeled as a free-standing multilayer film from the substrate with ease after immersion in pH 7.4 phosphate buffer overnight and light irradiation ($\lambda > 295$ nm for 1 h). The prepared free-standing film had a roughness of ≈ 5 nm and a thickness of ≈ 200 nm.

Based on hydrogen bonding, Xu *et al.*[95] developed a temperature-responsive sandwich-like membrane through the LbL technique using a block copolymer micelle (BCM) and hyaluronic acid. The BCM was synthesized by atom transfer radical polymerization using poly(*N*-isopropylacrylamide) (PNIPAM) and poly(2-hydroxyethyl methacrylate) (PHEMA) as shown in Fig. 3F. Block copolymer micelles with a PNIPAM core were deposited into the multilayer films (Fig. 3G) to introduce temperature sensitivity to the composite thin films. The multilayer films efficiently absorbed osimertinib—the third-generation inhibitor for lung cancer treatment. Even after several temperature-triggered swelling/deswelling (Fig. 3H) cycles, the films could retain

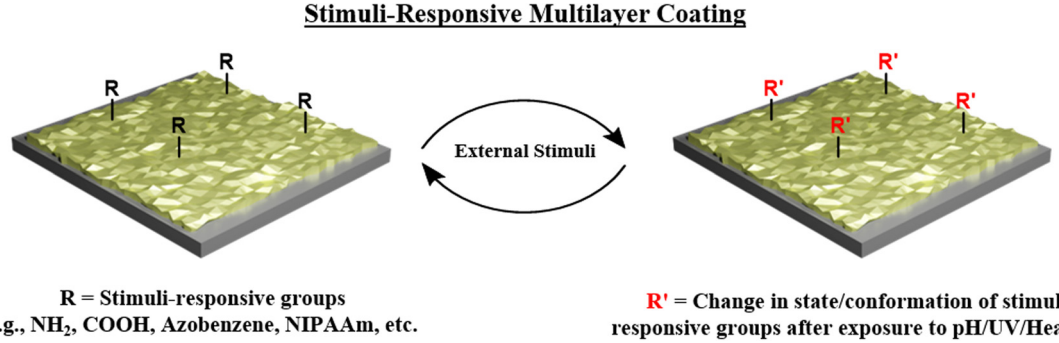

Fig. 2 Schematic representation of the stimuli-responsive coating/film with dynamic liquid wettability.

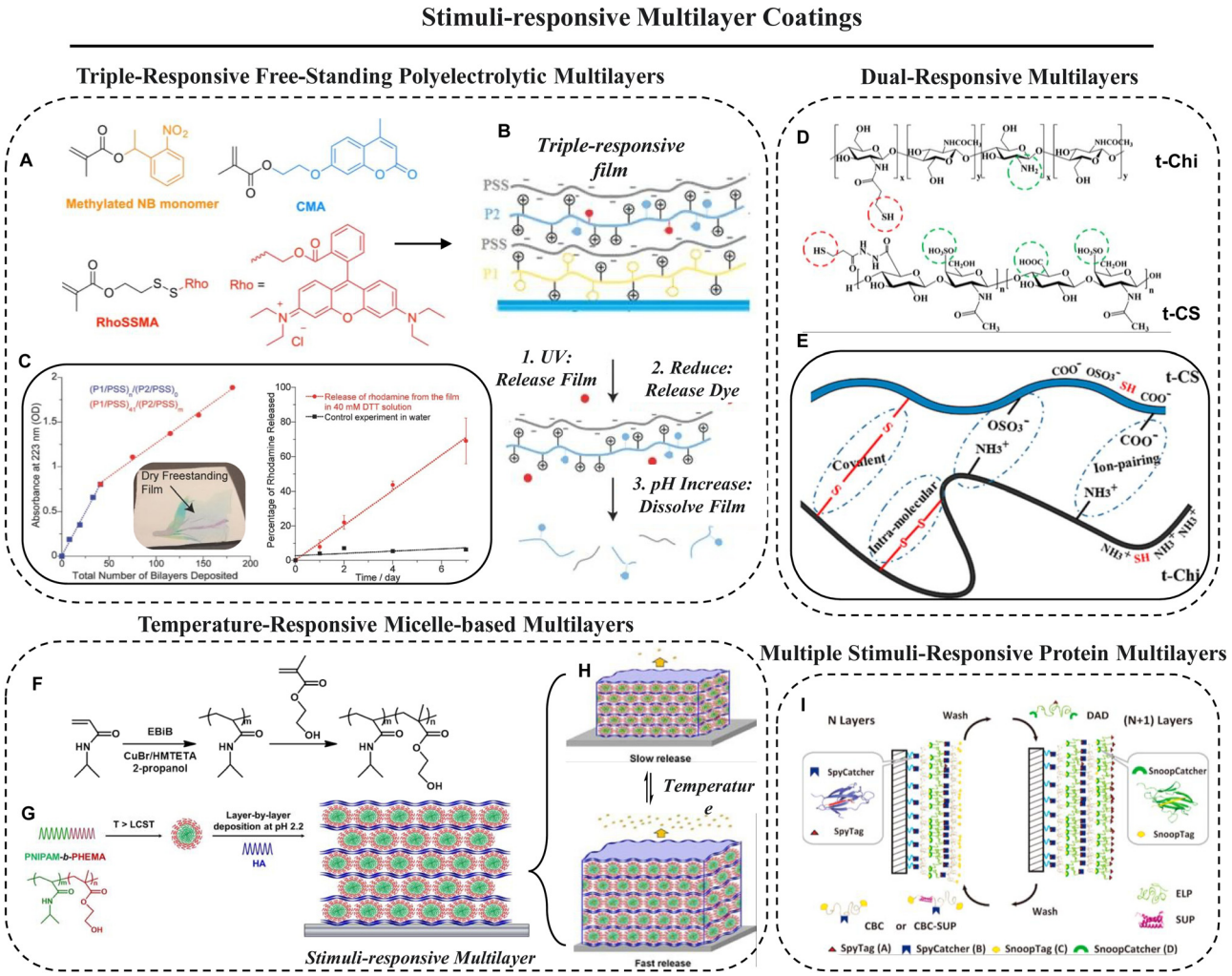

Fig. 3 (A) Chemical structures of monomers used in the preparation of the triple-responsive multilayer film. (B) Effect of three stimuli on the integrity of the film. (C) Effect of the number of bilayers on the absorbance of the film (the inset shows the free-standing film) and dependence of rhodamine release from the film with time. Reprinted with permission from ref. 94. (D and E) Representative structures (D) of thiolated chondroitin sulfate and thiolated chitosan where the circled groups indicate sites for ionic interaction (pH sensitive) and disulfide bond (redox sensitive) formation (E) in the multilayer coating. Reprinted with permission from ref. 97. (F–H) Synthetic procedure (F) for preparing a PNIPAM-based diblock copolymer, its deposition (after micellization) by the LbL technique to construct multilayer coatings (G) and release of the embedded molecule due to swelling of the multilayer coating triggered by surrounding temperature (H). Reprinted with permission from ref. 95. (I) Process of building all-protein-based multilayer coatings *via* orthogonal "Tag-Catcher" reactions without affecting the activity of proteins. Reprinted with permission from ref. 98.

their morphological integrity which was confirmed by ellipsometry measurements and atomic force microscopy.

Esmaeilzadeh *et al.*[97] established an LbL multilayer system of thiolated chondroitin sulfate (t-CS) and thiolated chitosan (t-Chi) (Fig. 3D), consisting of five double layers. Due to the presence of amino groups in t-Chi and carboxyl and sulfate groups in t-CS, the multilayer was pH-sensitive. In addition to that, the presence of free thiol molecules in both molecules made them redox-responsive. This multilayer assembly was carried out at acidic pH (4) to allow for ion-pairing between the negatively charged carboxyl and sulfate groups of CS and the positively charged amino groups of Chi. An increase in pH from 4 to 9.3 during layer formation and a chemical stimulus (chloramine-T) were used to verify the ability to cross-link the pendant thiol groups in the multilayer coating. The resulting multilayers exhibited stimuli-dependent behaviour upon both treatments, as demonstrated by thickness, topography, wettability, roughness, content of free thiols, binding of fibronectin, elastic modulus, and surface charge.

Zhang *et al.*[98] introduced two distinct LbL-derived protein based multilayer coatings *i.e.*, CBC/DAD (A, B, C, and D are SpyTag, Spycatcher, SnoopTag, and SnoopCatcher, respectively)[99] and CBC-SUP/DAD (super uranyl-binding protein is denoted as SUP). The selected ingridients were sequentially integrated on a silica gel surface using Tag-Catcher chemistry as shown in Fig. 3I. Such protein-based 2D multilayer (also denoted as biolayers) coatings exhibited responsive behavior to ionic strength, pH, temperature, and divalent ions like Ca^{2+} and UO_2^{2+}. Therefore, the multilayer was found to be highly efficient for uranyl sequestration from artificial seawater.[100]

Huang *et al.*[101] fabricated both pH- and salt-responsive chitosan/alginate dialdehyde (CHI/ADA) multilayer film through LbL multilayer deposition. The oppositely charged polyelectrolytes CHI and ADA interacted through electrostatic interactions, while the amine groups of CHI covalently cross-linked with the aldehyde groups of ADA. Further, the multilayer was post-chemically modified with sodium cyanoborohydride to avoid the dissociation of imine bonds under acidic conditions[102] by strategically transforming the dynamic imine bonds into permanent amine bonds.[103] Finally, this multilayer was extended for investigating its pH-responsive and multi-salt-responsive behavior along with its structural properties.

2.2. Chemically reactive multilayer coating (CRMLC)

Although stimuli-responsive materials are important for specialized applications, the design of durable multilayer coatings that would not be affected by changes in environmental conditions (*e.g.*, change in pH, ionic strength, temperature, *etc.*) is important for various other potential applications.[104–106] Approaches (*e.g.*, thermal treatment,[107,108] exposure to UV radiation,[109,110] or treatment with reactive cross-linking agents[111]) to introduce covalent cross-links to PEMs after fabrication have been developed to improve the stability of multilayers and to tune other important film properties such as compliance, stiffness, *etc.* Several groups have reported cross-linked multilayer coatings by either associating the direct covalent bond formation during the multilayer construction process or crosslinking the entire multilayer coating after the fabrication (Fig. 4).[112,113] These methods are typically based on covalent bond-forming reactions between polymers with suitable mutually reactive groups and, thus, lead to the formation of covalent cross-linking in the multilayer during the construction. The availability of two molecular building blocks with functionality that can easily form a covalent bond is the most basic requirement for these reactive processes.

In addition to increased durability of the multilayer, another major advantage of these reactive approaches is availability of residual reactive groups which can be used for further functionalization of these films (*e.g.*, post-modification with molecules that are able to react with these residual reactive groups). Though the surfaces of conventional PEMs (*e.g.*, ionically cross-linked) can be functionalized, advantages like chemical reactivity and increased film durability afforded by covalent assembly can facilitate modification after fabrication and can pave new ways for the design of functional interfaces with much better control over desired properties.[114] Such covalent modifications are achieved by employing various chemical reactions which are briefly discussed below.

Recently, the mutual reaction between thiol and ene groups (Fig. 5A) has offered unique advantages for postmodulating the chemistry of the prepared polymeric multilayer coating. This reaction stands out because it is photoinitiated, it is environmentally benign, and it can be performed at ambient temperature in the presence of oxygen.[115] Any potentially toxic metal catalysts are also not required in this process. Moreover, introducing functionality has become easier because of the vast array of commercially available biomolecules and molecules with either ene or thiol functionality.

The next one is the Schiff base reaction (Fig. 5B). This was first proposed by the German chemist Hugo Schiff in 1864[116] and is used widely due to its high reaction rates and mild reaction conditions.[117] In the context of multilayer formation, Schiff base bonding confers high stability to thin multilayers allowing them to withstand harsh conditions. Both aqueous and organic solutions can be chosen to perform such reactions.

LbL multilayer coating by using amidation chemistry was employed to prepare ultrathin nanocomposites on polyethylene films by Liao *et al.*[118] *via* covalently reacting appropriately selected ingredients, *i.e.* amine-functionalized multiwall carbon nanotubes and poly(methyl vinyl ether-*alt*-maleic anhydride) as an electrophilic component. The resulting multilayer coating exhibited superhydrophilicity with a WCA of $<10^{\circ}$. Upon covalent modification of the hydrophobic multilayer through the acylation process, the multilayer (as shown in Fig. 5C) became superhydrophobic and displayed a static WCA of 165°.

Another important reaction is mildly exothermic ring-opening that is generally observed between azlactone and aliphatic primary amines in the absence of any catalyst and under ambient conditions (Fig. 5D).[119] The carbon of the carbonyl group has the maximum electron deficiency in 2-alkenyl azlactone compounds where nucleophiles like amines can easily attack and open the azlactone ring. This type of facile chemistry has great potential as it can eliminate issues associated with conventional LbL techniques such as time-consuming processes, and poor stability due to insufficient bonding interactions between layers.

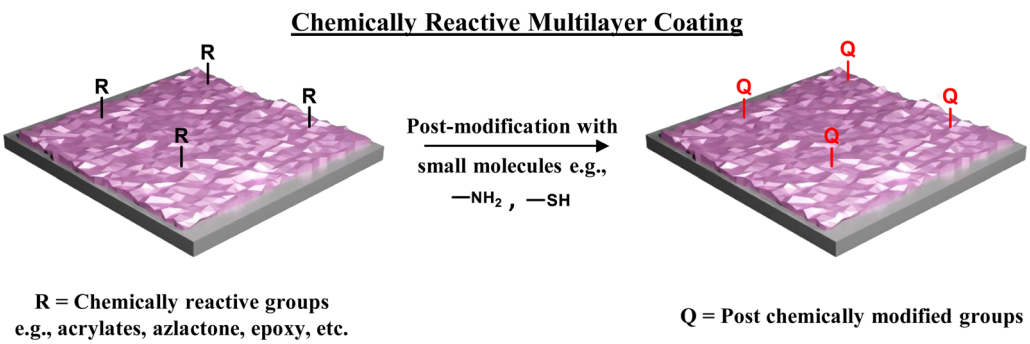

Fig. 4 Schematic representation of chemical modification of the 'reactive' covalently crosslinked multilayer coating.

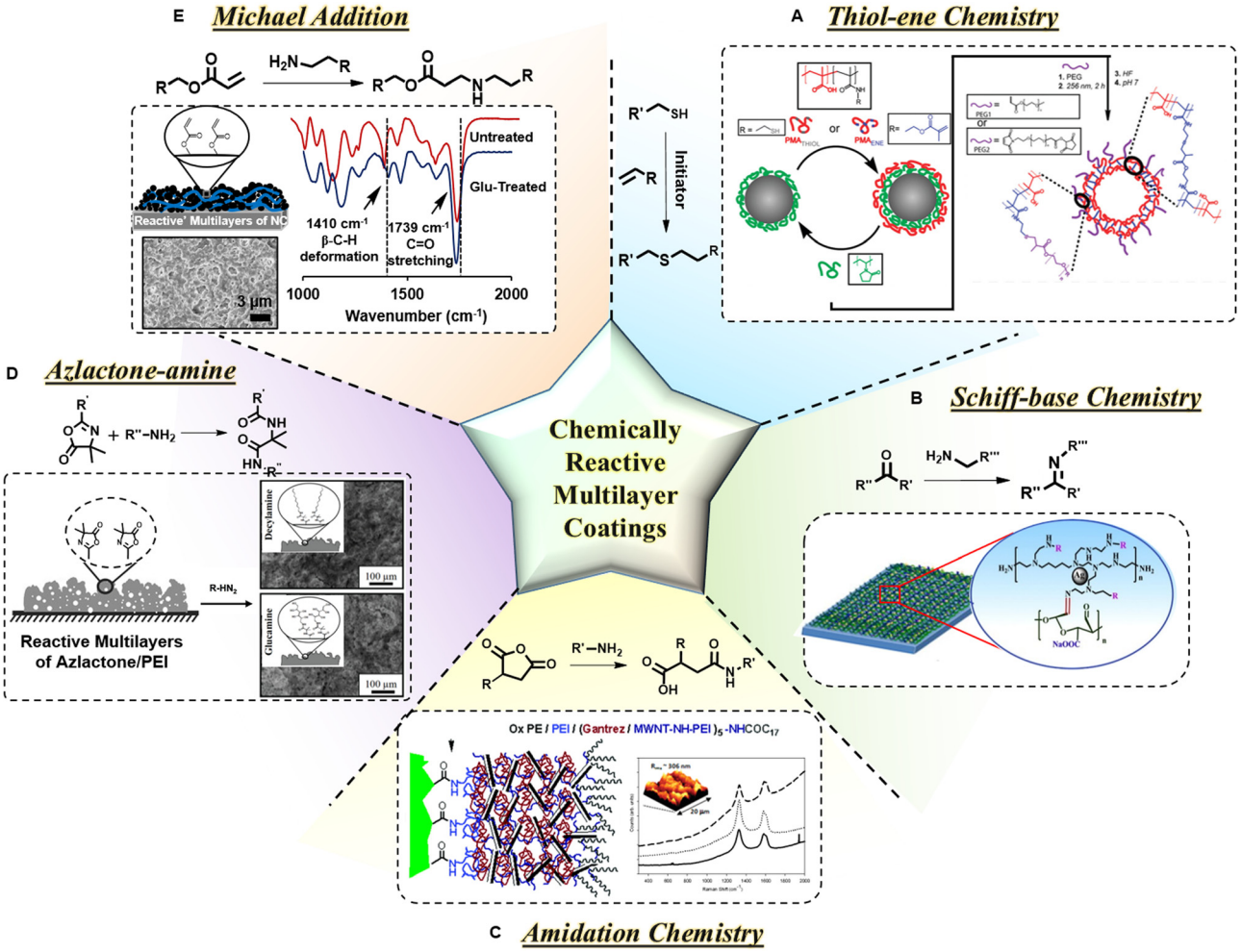

Fig. 5 Common reactions for fabrication/modification of 'reactive' multilayers. (A) Thiol–ene chemistry: preparation of (PVP/PMATHIOL/PVP/PMAENE)-coated particles and PEGylation and stabilization using thiol–ene chemistry, followed by removal of the silica template. Reprinted with permission from ref. 129. (B) Schiff-base reaction: Schematic illustration of the preparation of the covalently bonded LbL assembly by the reaction between aldehyde and amine moieties. Reprinted with permission from ref. 128. (C) Amidation chemistry: reaction of anhydride with the primary amine-containing molecule. Representation of the covalent LbL assembly after hydrophobization by post-acylation is provided. Reprinted with permission from ref. 118. (D) Azlactone–amine chemistry: schematic illustration and SEM images of the reactive PEI/PVDMA film after treatment with both decylamine and glucamine. Scale bars: 100 μm. Reprinted with permission from ref. 130. (E) Michael addition reaction: 1,4-conjugate addition reaction between primary amine and acrylate groups. A schematic illustrating the presence of residual acrylate groups. FESEM image of the 'reactive' multilayer of NC showing the morphology of the 20 bilayer coating. Comparative FTIR study on the untreated and glucamine-treated multilayer of NC to corroborate successful modification upon glucamine treatment. Reprinted with permission from ref. 10.

Among all of these chemistries, the Michael addition reaction (Fig. 5E) stands out owing to its numerous advantages: (a) reactivity in both liquid and solid phases, (b) mild reaction conditions, (c) catalyst-free approach, and (d) facile fabrication method.[86,87] The 1,4-conjugate addition of a readily reactive nucleophile to an α,β-unsaturated carbonyl moiety is mostly recognized as a Michael addition reaction which is very useful for carbon–carbon bond formation without the need for any harsh condition. During the reaction, a thermodynamically stable 1,4-conjugate addition product is formed *via* a resonance-stabilized enolate intermediate. The common nucleophiles (*e.g.*, amines, thiol, and phosphine groups) can readily participate in this addition reaction and form C–P, C–S, C–N, and C–O bonds through mutual Michael addition reaction.[86–88,120]

Multilayers with roughness in a few nanometers range are generally referred to as smooth. The smoothness of an interface can significantly affect the functional property of a multilayer due to the low surface area of smooth multilayers. For example, low surface area reduces the release of drug molecules as compared to rough multilayers that have higher surface area and can be of potential interest for controlled drug delivery.[121]

In contrast, porous and rough multilayers can be defined as multilayers with porous structures or with surface undulations in the hundred nanometers range or more, respectively. These multilayers have higher surface area as compared to smooth multilayers and different morphology altogether which alter their properties. Some reported porous/rough multilayer coatings/

films are highlighted for gaining more insight into their fabrication process and reactivity for incorporating dynamic properties.

Duan *et al.*[122] reported a facile fabrication of hemoglobin (Hb) spheres with high oxygen-carrying capability by using $CaCO_3$ particles as a decomposable template in combination with covalently crosslinked LbL of amine-containing Hb molecules and aldehyde-containing glutaraldehyde. Further, the Hb spheres underwent chemical modification with biocompatible polyethylene glycol (PEG) to prevent the leakage of Hb from the interior substrates and stabilize the system. Finally, 0.1 M Na_2EDTA (pH 7.0) solution was used for the removal of the $CaCO_3$ template, and the Hb spheres were obtained. Glutaraldehyde played a crucial role in covalent crosslinking through Schiff-base chemistry which inhibited the decomposition of Hb tetramers into dimers, prolonging its vascular retention and eliminating nephrotoxicity.[123,124]

The combination of LbL technique with Schiff base interaction results in the formation of a covalently cross-linked multilayer without any external additives.[125] This multilayer has been extended for the rapid development of highly durable functional films under ambient conditions.[117] The synthesis of the multilayer assembly involves reactive polymers containing aldehyde and amino groups leading to the efficient and orthogonal formation of imine bonds under physiological conditions.[126,127]

Xie *et al.*[128] explored the Schiff base reaction between an amine-containing zwitterionic polymer solution of PEI/sulfobetaine methacrylate (SBMA) and oxidized sodium alginate (aldehyde-rich) through an LbL deposition process to form an antifouling membrane with excellent anti-bacterial activity. This membrane was further loaded with silver nanoparticles (Ag NPs) through immersion of the membrane in silver nitrate ($AgNO_3$) solution by reducing $AgNO_3$. The combination of zwitterionic polymer consisting of covalent multilayers and the chelated AgNPs on the membrane surface (Fig. 5B) resulted in both bulk anti-bacterial and surface anti-fouling properties. PEI-SBMA adhered on the surface of the membrane to functionalize with OSA followed by *in situ* generation of Ag NPs by chelating the Ag ions led to the development of anti-fouling and anti-bacterial properties. By increasing the number of layers, the bactericidal property was improved.

Connal *et al.*[129] reported a method to construct a stable LbL capsule by light-assisted thiol–ene click chemistry (Fig. 5A). The hydrogen-bonded LbL assembly was fabricated by alternately depositing poly(methacrylic acid), that was decorated with either ene or thiol groups, and poly(vinylpyrrolidone) on silica particles at pH 4. PMA was strategically modified with ene or thiol moieties using carbodiimide coupling reaction. Upon exposure to UV light (256 nm) for 2 hours, radicals from thiol group initiate a radical addition reaction across the double bond of the methacrylate moiety and providing the needed stability to the multilayer. The multilayers could further undergo thiol–ene reaction with ene-end functional PEG to generate a low fouling and reactive polymeric multilayer.

Manna *et al.*[130] developed a bulk superhydrophobic coating through LbL deposition of PVDMA and PEI, which involved alternate dipping in respective polymeric solutions 600 times and resulted in only 80 μm thick film after 100 bilayers of deposition. These multilayered PEI/PVDMA coatings were found to be inherently associated with hierarchical and porous topography—which is essential to achieve superhydrophobicity. The azlactone-containing PEI/PVDMA multilayers (having a thickness of ~80 μm) were treated individually with D-glucamine (a model hydrophilic amine) and *n*-decylamine (a model hydrophobic amine) to associate distinct and desired water wettability (Fig. 5D).

Avila-Cossio *et al.*[131] used this chemistry to prepare a polymeric film (35 and 35.5 bilayers) through covalent cross-linking of PVDMA and PEI. The presence of residual amine groups from PEI was confirmed by ATR-FTIR and made the multilayer reactive which helped in desired immobilization of various fatty acids (palmitic acid, lauric acid, and myristic acid). The effect of functionalization with fatty acids was investigated in order to assess their impact on the proliferation and adhesion of Langerhans β-cells.

In the recent past, Ford *et al.*[132] synthesized a covalently cross-linked multilayer coating through Michael addition reaction of BPEI (branched polyethyleneimine) with small multifunctional acrylate *via* consecutive deposition by adopting the LbL process. Later, Bechler *et al.*[133] extended this LbL coating to achieve a porous 'chemically reactive' polymeric multilayer with a thickness of 750 nm. Post-modification with amine-containing small molecules was enabled by the residual acrylate functionalities in the developed multilayer. The facile reaction between the acrylate group and the primary amine moiety can be held responsible for the reactive nature of the multilayer.

A 'reactive' multilayer of a nanocomplex was prepared by Parbat *et al.*[10] through covalent crosslinking between amine groups of BPEI and acrylate groups of the prepared reactive nanocomplex (NC) through sequential 1,4-conjugate addition reaction. The prepared material could retain its properties in physically and chemically harsh environments due to the existence of covalent cross-linking through Michael addition reaction. After the construction of 20 bilayers (each layer was formed by the sequential deposition of the reactive NC and the polymer (BPEI)), a chemically reactive coating loaded with residual acrylate groups was formed. Investigation of the as-prepared and post-modified multilayer by FTIR confirmed the existence of residual reactive groups and their ability to react with appropriately selected small molecules.

Parbat *et al.*[134] extended this work to fabricate a multilayer-coated stretchable fibrous substrate with superoleophobicity under water. 1,4-conjugate addition reaction between the branched polymer and multiacrylate formed a covalently bonded network on the fibrous matrix. The prepared coating remained mechanically durable as the prepared material exhibited unaltered bio-inspired wettability even after application of a high tensile strain (up to 150%).

Therefore, it can be concluded from the above discussion that the appropriate use of these CRMLCs based on the covalent cross-linking chemistries has a lot of potential for developing various advanced materials/interfaces associated with distinct and relevant properties.

3. Applications of 'stimuli-responsive' and CRMLCs in developing functional interfaces

Functional multilayers prepared by the LbL self-assembly technique have attracted great attention recently because of their wide applications in areas including sensors, nanoreactors, drug delivery, nonlinear optics, and antireflective films.[135] Stimuli-responsive multilayers were reported in the early stage of the development of dynamic functional interfaces, but these were mostly fabricated by depositing oppositely charged polyelectrolytes alternatively. Such construction through electrostatic interactions inherently suffered from poor stability in various chemical environments and when subjected to physical manipulations. Later on, many multilayers were reported with covalent linkages to improve the stability of films in various chemical environments. Even after this improvement, the flexibility to modify the materials chemically in order to control the functional property is limited. Therefore, such stimuli-responsive multilayers have limited scope as far as practical applications are concerned. The conceptualization of chemically reactive multilayers can overcome this challenge. CRMLCs have adequate reactive groups which can undergo facile reactions with suitable functional groups, and thereby, it becomes easier to modulate the desired property for intended application.

3.1. LbL coating with self-healing properties

The initial concept of self-healing properties of multilayers was suggested by Elender *et al.*[136] Self-healing materials are capable of repairing the damage caused by mechanical stress over time. Because of lower production costs and their long lifetime, the demand for self-healing materials is on a rise.[137] Among various self-healing materials, self-healing coatings capable of protecting (against corrosion or damage) the underlying substrates and endowing the substrate with the desired property are the most sought-after.[138] In recent scientific investigations, it has been shown that LbL assembly is highly promising for developing self-healing coatings.[139]

Because of the sensitivity of the electrolytic building blocks to external stimuli, LbL self-assemblies have inherent potential to be considered as dynamic coatings. The damaged surfaces can be mostly healed by the formation of new chemical bonds (covalent or non-covalent) upon exposure to external stimuli. One basic criterion for self-healing is that the polymer chains should have sufficient mobility to diffuse into the damaged areas and to facilitate the formation of new chemical bonds by bringing reactive groups closer to the damaged region.

Cui *et al.*[140] developed LbL films of branched PEI/PAA with the inclusion of various types of latex particles (butyl acrylate/methyl methacrylate/2-hydroxyethyl methacrylate (HEMA) was used to prepare the latex particles) with different T_g and different compositions. The incorporation of latex particles weakened the interaction between BPEI and PAA and introduced free volume during film assembly, and allowed for greater mobility of the polymer chains. Due to the hydrophilic properties of HEMA, among the particle-containing films, the swelling ratio increased when the latex particles in the films were composited with more HEMA. The water uptake behaviour of the films can elucidate the reasons for different self-healing performances in water. Water acts as a plasticizer and increases the mobility of the polyelectrolyte chains. Therefore, water-responsivity and steam-enabled self-healing of these films were observed (Fig. 6A–C). The films with various latex particles exhibited different swelling ratios, surface hydrophilicity, as well as ability to self-heal scratches.

Manna *et al.*[141] reported an approach for self-healing of crushed polymeric superhydrophobic coatings by recovery of damaged micro- and nanoscale topographic features. The porous polymer multilayers ($\sim$80 μm thick) were fabricated by the 'reactive' LbL assembly (Fig. 6D) of BPEI and the amine-reactive polymer PVDMA. These PEI/PVDMA multilayers were covalently crosslinked (owing to the formation of amide/amide-type bonds that formed during assembly) and they contained residual amine-reactive azlactone groups that could be used to immobilize secondary functionality. Upon reaction with the hydrophobic small molecule *n*-decylamine, these films became superhydrophobic. They demonstrated that the application of crushing loads to porous superhydrophobic films severely compacted the coatings and completely flattened the micro/nanoscale features as shown in Fig. 6E–H, but after treatment with liquid water, these features could be recovered. The use of water as a restorative agent was counterintuitive in this context, but led to revive films that were virtually indistinguishable, in both form and function, from the original coatings prior to crushing. Crushing and healing were performed multiple times on these coatings using the water-assisted approach and this aqueous crush/recovery process was extended to pattern the surfaces of these superhydrophobic multilayers with water-soluble agents.

A self-healable adhesive actuating material was demonstrated by Gu *et al.*[142] by taking advantage of the solvent-responsive behaviour of weak polyelectrolyte multilayers consisting of BPEI/PAA followed by another 50-bilayer deposition of PDAC/SPS (polystyrene sulfonate) as shown in Fig. 6I and J. Dehydrated multilayers were obtained upon contact with an organic solvent which became sticky upon wetting with water. Exposure to ethanol significantly contracted the PEM indicating that the asymmetric structure as a whole curled in response to this stimulus and then returned to a levelled film when ethanol is removed due to evaporation and rehydration of the multilayer (Fig. 6J). The removal of water closely bound to the PE chains resulted in strengthening of the interactions between polymer backbones within the film and therefore, contraction of the film. An asymmetric heterostructure consisting of a responsive PDAC/SPS multilayer block and a nonresponsive BPEI/PAA component displayed actuation when exposed to ethanol. The curl degree of the prepared material was found to be as high as $\approx$228.9° (Fig. 6K).

3.2. LbL coating with antimicrobial properties

Biofouling, *i.e.*, the accumulation of micro/macro-organisms on various surfaces, has been extensively addressed due to its

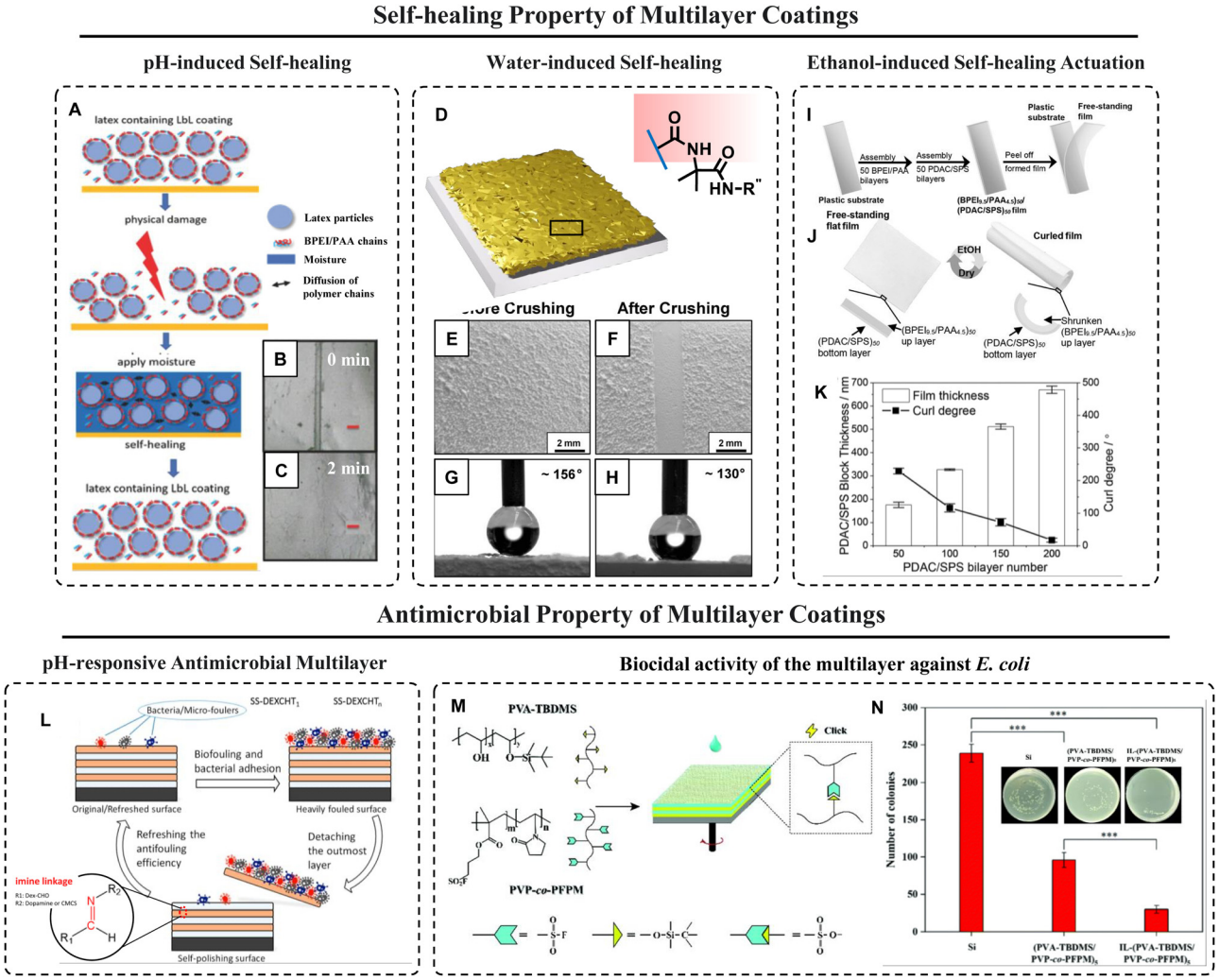

Fig. 6 (A) Schematic representation of the water-assisted self-healing process of the latex-containing PEMs. (B and C) Optical micrographs of the multilayer after scratch (B) and after healing (C). Reprinted with permission from ref. 140. (D–H) Pictorial representation and chemical structure of the porous multilayer (D) constructed by PVDMA and BPEI, and recovery of topographic features (E and F) as well as superhydrophobicity (G and H) of the crushed multilayer by treatment with water. Reprinted with permission from ref. 141. (I and J) Depiction of the preparation of a free-standing multilayer film (I) and its ability to switch between flat and curl state repeatedly (J). (K) Illustration of the effect of bilayer number and coating thickness on curl degree when treated by pure CH_3CH_2OH. Reprinted with permission from ref. 142. (L) Depicting the antifouling behaviour through the self-polishing mechanism of the multilayer coating on the SS surface under acidic conditions. Reprinted with permission from ref. 143. (M) Illustration of preparation of the spin-assisted multilayer coating along with the selected building blocks and their interactions/bondings. (N) Digital images of agar plates with MG1655 strain of *E. coli* treated with the control silicon substrate and prepared multilayers and the plot shows biocidal activity by the colony counting method. Reprinted with permission from ref. 144.

ecologic and economic consequences. Adequate functionalization and modification of the surface *via* molecular design are employed to impart substrates with anti-adhesion and antimicrobial efficacies. In the LbL approach, surfaces can be fabricated and modified easily as it allows control of the chemistry, thickness, and morphology of films, and thereby, adequate functionality can be incorporated and tuned as per the intended application.

Xu *et al.*[143] reported LbL multilayer coating using carboxymethyl chitosan (CMCS) and dextran aldehyde (Dex-CHO) through imine linkages. One bilayer deposition of a mussel adhesive-inspired polydopamine (PDA) layer followed by deposition of the dextran aldehyde (DEX) layer *via* aldehyde–amine reaction on the stainless steel (SS) surfaces was completed. The antifouling and antimicrobial adhesion efficacies of the multilayers were demonstrated and evaluated against bacterial adhesion (both Gram-positive and Gram-negative bacteria), protein adsorption (bovine serum albumin, BSA), and microalgal attachment (*Amphora coffeaeformis*). The self-polishing ability of the coatings was achieved by exposure to the acidic environment which allowed the cleavage of pH-responsive imine linkages. Thus, the efficacies of antifouling and antimicrobial adhesion were enhanced by the self-polishing ability of the multilayers (Fig. 6L).

Liu *et al.*[144] developed covalently bonded reactive polymeric multilayer films by spin-assisted LbL deposition through "sulfur(VI)-fluoride exchange" (SuFEx) click reaction which is

a high-yield reaction between a sulfonyl fluoride (–SO_2F) group or a fluorosulfate (–OSO_2F) group and a silyl ether. A silyl ether-rich polymer, *tert*-butyldimethylsilyl-modified polyvinyl alcohol (PVA-TBDMS), and a sulfonyl fluoride-rich polymer, poly(*N*-vinyl-2-pyrrolidone)-*co*-poly(3-(fluorosulfonyl)-propyl methacrylate) (referred to as PVP-*co*-PFPM), were chosen for the formation of multilayer coating (Fig. 6M). The stability of multilayer-coated silicon substrates was evaluated by soaking the samples in saline (1 M phosphate-buffered saline and 1 M NaCl) and acidic (0.1 M HCl) aqueous solutions at room temperature for 4 hours. The IL-functionalized (PVA-TBDMS/PVP-*co*-PFPM)$_5$ film showed a strong biocidal activity (Fig. 6N) with ~87% cell death due to the strong bactericidal activity of imidazolium-type ionic liquids.

Nyström *et al.*[145] formed a microgel multilayer by a straightforward LbL deposition approach based on biotin-conjugated poly(ethyl acrylate-*co*-methacrylic acid) (MAA) microgels and avidin, incorporating antimicrobial peptide KYE28 in a step-wise manner during the multilayer build-up process. Incorporation of the antimicrobial peptide KYE28 into the microgel multilayers was achieved either in one shot after multilayer formation or through addition after each microgel layer deposition. Further, the antimicrobial properties of the peptide-loaded microgel multilayers against *E. coli* were investigated and compared to those of a peptide-loaded microgel monolayer.

3.3. LbL coating with superhydrophobic properties

Superhydrophobic surfaces inspired by highly exceptional natural designs like ''lotus leaf'' have been researched extensively due to their various applications. Two important factors, *i.e.*, appropriate roughness of the surface and low surface energy coating on the top, contribute to such superhydrophobic structures, leading to the development of artificial super-hydrophobic surfaces with controlled modulation of wettability.[146] LbL assembly is a versatile and reliable method for the fabrication of composite films with precisely controlled film structures and composition.[147] The conventional thin LbL superhydrophobic interface that is achieved through optimization of essential chemistry on top of the hierarchically featured interfaces—by associating delicate chemistry—is less appropriate for sustaining various severe challenges in practical settings. This limitation was addressed by introducing chemically reactive porous multilayer coatings.

Zong *et al.*[148] reported a facile dip-coating approach to fabricate a cotton fabric-based photo-responsive surface with rapid photo-switchable wettability, guided by the combined effects of the conformational variation of fluorine-containing azobenzene chemistry and the inherent porous hierarchical features of the fabric. Owing to the surface decorated with designed acrylate copolymers bearing a trifluoromethyl side chain and fluorine-containing azobenzene derivative moieties, the modified fabric possessed rose petal-like superhydrophobicity with a large contact angle (WCA $\approx 150^\circ$) as well as high water adhesion. This as-prepared fabric was capable of rapid switching of wettability between superhydrophobicity and superhydrophilicity *via* simple alternate ultraviolet (UV)/visible light irradiation (Fig. 7A).

Parbat *et al.*[149] introduced a salt-assisted multilayer of a reactive NC *via* accelerated growth of a chemically reactive polymeric coating (Fig. 7B) in the presence of sodium chloride salt. Both superhydrophobicity and underwater superoleophobicity were achieved on various flexible and rigid substrates (including wood, Al-foil, synthetic fabric, *etc.*) by the consecutive deposition of salt-assisted 9 bilayers of NC and BPEI followed by appropriate post-covalent modifications. This facile and simple LbL fabrication strategy is efficient in tailoring various other liquid wettabilities both in air and under water, along with extremes of liquid (water and oil) wettability. This design allowed independent investigation of the essential physical and chemical parameters that conferred heterogeneous wettability for beaded water and oil droplets on respective solid surfaces.

Carter *et al.*[150] reported an approach for the functionalization of covalently crosslinked and physically stable azlactone-containing PEI/PVDMA multilayers using primary alcohol-, thiol-, and hydrazine-based nucleophiles as shown in Fig. 7C. The residual azlactone groups in the polymer multilayer fabricated by the reactive LbL assembly of PVDMA and branched PEI reacted with amine-based nucleophiles to dictate new interfacial and bulk properties through the creation of chemically stable amide/amide-type bonds. Different lengths of alkyl chains with amine were incorporated into the multilayer to tune the wettability and hydrophobicity of the film. The azlactone groups of these covalently crosslinked materials could also be functionalized using less nucleophilic alcohol- or thiol-containing compounds, using an organic catalyst, or converted to reactive acylhydrazine groups by direct treatment with hydrazine. The ester, acylhydrazine, and thioester groups that resulted from these reactions can be cleaved under mild conditions in aqueous environments, leading to dynamic and responsive materials that can release covalently bound molecules into surrounding media or undergo changes in extreme wetting behaviours that cannot be achieved using coatings functionalized with primary amines.

3.4. LbL coating with underwater superoleophobic properties

Underwater superoleophobic materials can extremely repel oil/oily phases (with an advancing oil CA $\geq 150^\circ$ and CAH $< 10^\circ$) under water.[151] Synthesis of such fish-scale-mimicked[9] underwater superoleophobic coatings is of potential interest in diverse applied contexts.[152] The versatility of the LbL coating allows the construction of functional materials with highly tunable architectures and properties, and is therefore used as a universal technique for fabricating underwater superhydrophobic surfaces.[153]

Parbat *et al.*[10] reported a LbL multilayer coating of a chemically reactive, polymeric nano-complex (NC) exploiting the Michael addition reaction between the amines and acrylates of BPEI and 5Acl, respectively (Fig. 7D). This work was discussed earlier for studying residual chemical reactivity using the FTIR technique. 5Acl molecules acted as a cross-linker during the facile reaction and formed a nanocomplex as the reaction progressed. The synthesized multilayer had numerous advantages such as high chemical/physical durability due to covalent cross-linking, greater optical transparency (Fig. 7G), and the ability to coat

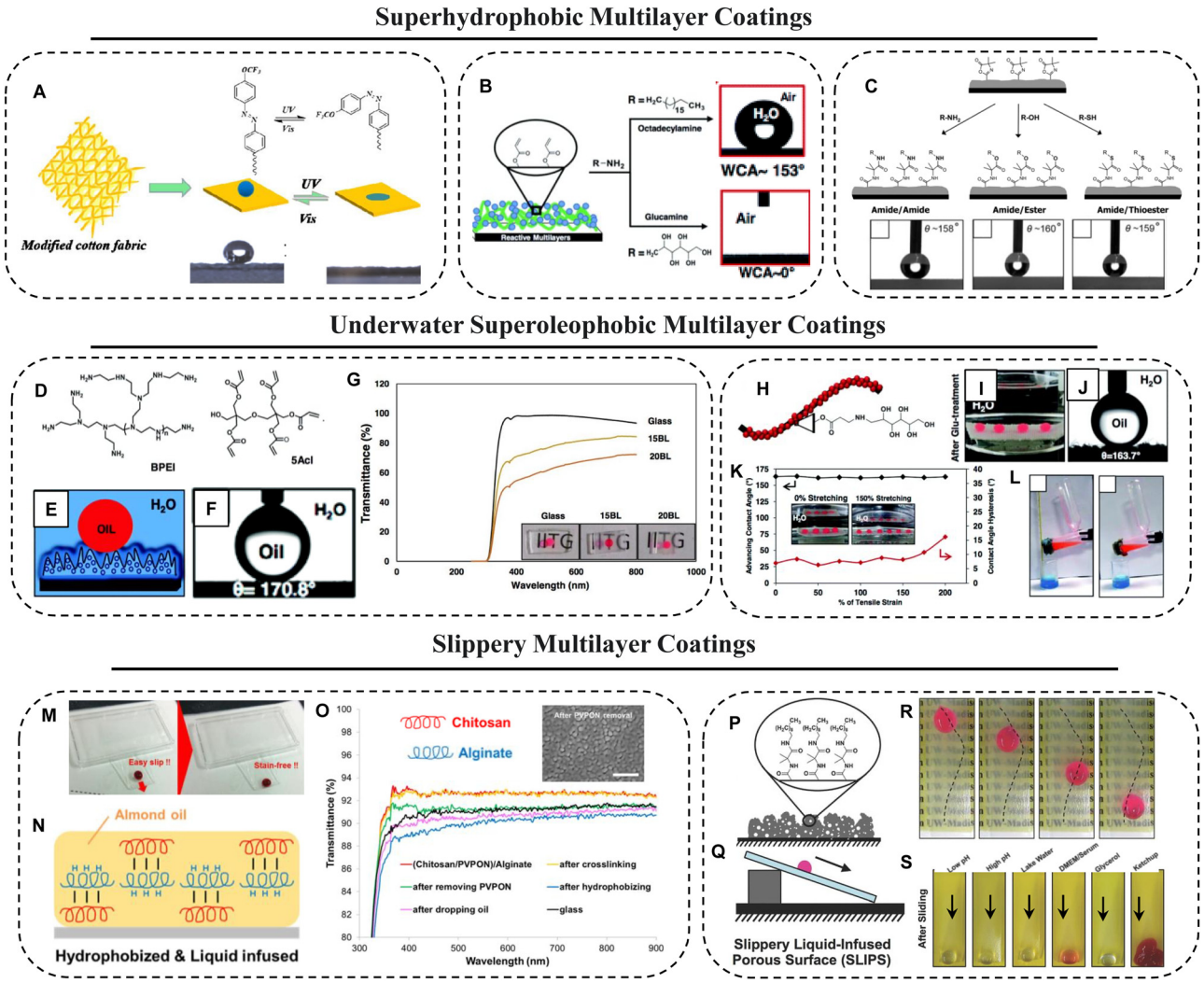

Fig. 7 (A) Reversible change in wettability of the azo-copolymer coated cotton fabric surfaces upon exposure to UV and visible light. Reprinted with permission from ref. 148. (B) Schematic representation of the multilayer constructed by NCs (prepared in the presence of NaCl) and BPEI polymer and CA images of beaded water droplets on the multilayer after post chemical modification with ODA and glucamine molecules. Reprinted with permission from ref. 149. (C) Illustration of the chemical structures of residual azlactone moieties in the PVDMA/PEI multilayer and the modification of these azlactone groups by nucleophiles containing amine, alcohol or thiol groups. Modification with nucleophiles with long chains made the multilayers superhydrophobic. Reprinted with permission from ref. 150. (D and F) Chemical structures (D) of the building blocks of the multilayer, *i.e.* dipentaerythritol penta-acrylate (5Acl) and branched poly(ethylenimine) (BPEI). Illustration (E) and CA image (F) of the multilayer after modification with glucamine. (G) Plot exhibiting % transmittance of multilayer coated (after post-modification with glucamine) and uncoated glass substrates. Reprinted with permission from ref. 10. (H–L) Illustration of covalent post-modification of the multilayer with glucamine. Digital (I) and CA images (J) of beaded oil droplets under water on post-modified coated fabric. Reprinted with permission from ref. 134. (M and N) Digital images (M) and schematic representation (N) of the slippery chitosan–alginate multilayer coating infused with almond oil. (O) The FESEM image depicting the porous behavior of the multilayer and the plot showing % transmittance of the prepared multilayer at various stages of slippery coating preparation. Reprinted with permission from ref. 157. (P and Q) Illustration of the decylamine modified PVDMA/PEI multilayer (P) and slippery behavior (Q) of this multilayer after oil-infusion. (R and S) Demonstration of the guided sliding (R) of a water droplet on the developed SLIPS and sliding (S) of various complex media on the SLIPS-coated glass substrate. Reprinted with permission from ref. 13.

various substrates. This design was further extended to reveal the basis of the extremes of oil-wettability under water in detail. The continuous (for underwater superoleophobicity), and discontinuous (for underwater superoleophilicity) three-phase contact lines (TPCLs) were acheived just by post-modifying the 'reactive' multilayer with appropriate chemistry, which enabled one to precisely modulate the underwater oil-wettability on solid surfaces as shown in Fig. 7E and F.

The above chemistry was extended further to develop a highly stretchable (150% strain) and durable underwater superoleophobic membrane (Fig. 7H–J) through strategic integration of the 'reactive' multilayer coating with an inherently stretchable fibrous polyurethane substrate.[134] The as-prepared membrane embedded with bio-mimicking wettability (advancing oil CA ~ 162°) remained intact under diverse harsh physical, chemical, and mechanical conditions like different physical abrasion tests,

prolonged exposure (30 days) to UV irradiation, exposure to high and low temperatures (100 °C and 10 °C), successive (1000 times) tensile deformations with 150% tensile strain (Fig. 7K), and exposure to severely complex aqueous phases. The as-synthesized material was used to demonstrate gravity-driven and environmentally friendly cleaning of various types of oil spillages (Fig. 7L) under severe physical/chemical conditions.

3.5. LbL coating with slippery properties (SLIPS)

Aizenberg and co-workers[154] introduced the fundamental basis behind the slippery liquid-infused porous surfaces (SLIPSs) in 2011 through the strategic infusion of perfluorinated liquids into nanofibrous Teflon on membranes. SLIPSs are inspired by *Nepenthes* pitcher plants that exhibit robust anti-fouling behaviour.

Unlike lotus-leaf-mimic surfaces, SLIPSs consist of a thin and moveable lubricant layer that is spontaneously drawn into the porous features leading to a continuous replenishment of the damaged area by capillary forces. SLIPSs allow other liquids (like oil or water phases) placed in contact to slide off readily with sliding angles as low as 2°. Continuous retention and restoration of thin films of oil in the featured interfaces help in maintaining the slippery behaviour, depending on the chemical compatibility between the infused oil phase and the matrix revealing design criteria that can be exploited to manipulate the behaviours of contacting fluids (*e.g.*, modulation of sliding angles and velocities[155] or creation of responsive surfaces that allow control over interfacial behaviours).[156]

Due to its several advantages, *e.g.*, applicability to any solvent-accessible surface, simple fabrication process, better control over surface morphology, *etc.*, LbL assembly is considered as one of the most efficient techniques to develop SLIPSs.

Manabe *et al.*[157] fabricated a non-fluorinated SLIPS (Fig. 7M) with a biodegradable and biocompatible film by using PVPON, sodium alginate, and chitosan through H-bonding and electrostatic LbL assembly.[158] The PVPON was removed to create porosity by utilizing the pH-sensitivity of hydrogen bonds by exposing the cross-linked alginate and chitosan film to a buffer solution of pH 10. After methyl silanization of the surface, biocompatible almond oil (Fig. 7N) was used to cover the film surface. The durability of the material in the environment was investigated for 30 days and it could maintain ~90% transmittance throughout as shown in Fig. 7O.

Manna *et al.*[13] designed an oil-infused slippery interface by using a chemically reactive multilayer coating fabricated through LbL assembly of PVDMA and BPEI followed by modification with decylamine (Fig. 7P). The micro/nanoporous morphologies containing voids and other features could trap and host the liquid phase (an oil phase was used here to prepare SLIPSs). The physically/chemically durable SLIPSs (Fig. 7Q) were developed on various hard or soft substrates (*e.g.*, plastic, Al foil, *etc.*) of arbitrary shape, size, and topology. In comparison to the conventional design of a slippery multilayer, the chemically reactive multilayer provided a platform to tune the interactions of the matrix with the infused oil phase. The silicone oil-infused multilayer coating was found to be stable and slippery (Fig. 7S) under a wide range of chemically complex conditions including extreme pH conditions, ketchup, serum-containing cell culture medium, and unfiltered eutrophic lake water *etc*.

3.6. Other functional surfaces

3.6.1. Surfaces with photo/electrothermal properties. Heterostructured architectures of photo/electrothermally active multilayers are highly promising for energy, separation, electromagnetic interference shielding, *etc.*[159]

Zhou *et al.*[160] prepared a LbL assembly on a bacterial cellulose (BC) substrate by repeated spray coating of cellulose nanofiber and $Ti_3C_2T_x$ nanocomposites. Because of the Joule heating phenomena, the surface temperature could be increased based on the applied voltage. This film could attain the temperature of 50 °C, 90 °C, and 130 °C at 2 V, 3 V, and 4 V, respectively. This film was also able to exhibit photothermal behaviour. The surface temperature of this film reached 90 °C only after exposure to one sun irradiation (~1000 W m^{-2}) for 300 s. This heating and cooling cycle could be repeated multiple times without any change in performance.

3.6.2. Biosensing. LbL multilayers with suitable topography and surface chemical modification are widely utilized in labelling, biosensing, and targeted drug delivery.[161]

Zhao *et al.*[162] reported a polyelectrolytic multilayer membrane *via* LbL deposition of positively charged PDDA-protected Prussian blue nanoparticles and glucose oxidase (GOx) on a modified gold (Au) electrode surface. This multilayer was utilized as a biosensor and exhibited good selectivity for glucose sensing which was determined by the electrocatalytic reduction current of H_2O_2 produced in the presence of oxygen and glucose.

Recently, a dually reactive multilayer coating was reported by Borbora *et al.*[18] and this multilayer is novel because of its unique ability to participate in cooperative assembly with amphiphiles without compromising UW superoleophobicity, but oil adhesion. The interplay among the pH of the aqueous media, the molecular structure, and the concentration of the amphiphiles was mainly responsible for the reversible change in the oil adhesion of these multilayers. These multilayers were demonstrated to be highly efficient by the naked eye as well as by real-time identification of the charge of ionic surfactants and the concentration of biological molecules, *i.e.*, bile acids. The presence of different interfering agents had an insignificant effect on the sensing ability of the developed multilayers.

3.6.3. Surfaces with actuation properties. The LbL technique possesses immense potential in fabricating different polymer actuators. However, this particular application of multilayer coatings is hardly explored to date. Ma *et al.*[163] introduced a humidity-responsive walking device with a polyelectrolytic multilayer film consisting of PAA/PAH and UV-curable adhesive. This multilayer actuator was able to carry a load 120 times its own weight and walk steadily under periodic alternation of the relative humidity between 11% and 40%. The cross-linked PAA/PAH layer was capable of adsorbing/desorbing water depending on the humidity of the surroundings, respectively resulting in swelling or shrinking of the as-prepared films.

Song *et al.*[164] reported a multilayer membrane fabricated *via* stacking two LbL systems (polyurethane (PU)/PAA) and PEI/PAA with distinct swelling behaviour in aqueous and organic vapor. Each multilayer system was assembled through complementary electrostatic interaction between the oppositely charged functional moieties (*i.e.*, $-NH_2$ and –COOH). The precise control over the thickness ratio of the PEI/PAA and PU/PAA layers guided the degree of bending/curling of the membrane. Due to the dissimilar actuating behaviour in water and methanol vapors, this multilayer membrane exhibited fast and reproducible environmental detection.

4. Conclusion

In this review, we have presented some important glimpses of the LbL technique and its strategic uses in developing functional interfaces. This method provided a simple basis to precisely control both the structure of the coating and thickness even at nanoscale accuracy. Additionally, different materials with desired properties can be developed by incorporating adequate chemical functionalities during or after multilayer construction. In the past, the LbL approach has drawn significant attention due to its various applications discussed in the respective sections of this review. Here, we have accounted multilayer coatings that were associated with either stimuli-responsiveness or residual chemical reactivity. The conventional multilayer coatings that are constructed through weak chemical bonding and interactions generally suffered from durability issues. In the past, some attempts were made to improve the stability of such multilayer coatings by the association of chemical cross-linking, but achieving the desired post-chemical modifications remained challenging with these conventional multilayer coatings. As an alternative, the reactive multilayer coating was introduced to overcome the limitations of (a) durability and (b) desired post-covalent modifications. In the past, various covalent chemistries like thiol–ene reactions, Schiff base reaction, Michael addition reaction, *etc.* were successfully applied for (i) associating adequate durability to the prepared coating and (ii) achieving residual chemical reactivity to modify the prepared coating with desired chemical functionalities. Due to these advantages, the reactive coatings are highly suitable for fabricating various interfaces with desired functionalities having potential use in various research topics. The design of stimuli-responsive and chemically reactive LbL coatings is a multifaceted approach that has the power to overcome the limitations of the use of various functional interfaces in practically relevant applications. This offers a wide range of options to design new structural and multi-functional materials used for drug delivery, biomedical applications, anti-corrosion, oil–water separation, robotics, *etc.*

Conflicts of interest

There are no conflicts to declare.

Acknowledgements

The financial support from the Ministry of Electronics and Information Technology (no. 5(1)/2022-NANO) and DBT (BT/PR45283/NER/95/1919/2022) is acknowledged. U. M. thanks the Alexander von Humboldt Foundation for the Humboldt research fellowship (Humboldt-ID: 1216042) for experienced researchers. We acknowledge the generous support from the Department of Chemistry, CIF, CFN, SHST and Indian Institute of Technology-Guwahati.

References

1 C. Jiang and V. V. Tsukruk, *Adv. Mater.*, 2006, **18**, 829–840.
2 C. Shao, Y. Liu, J. Chi, Z. Chen, J. Wang and Y. Zhao, *Langmuir*, 2019, **35**, 3832–3839.
3 W. Wright and O. Wright, *US Pat.*, 821393A, 1906.
4 H. Izumia, M. Suzukia, S. Aoyagia and T. Kanzaki, *Sens. Actuators, A*, 2011, **165**, 115–123.
5 G. D. Mestral, *US Pat.*, 2717437A, 1955.
6 W. Barthlott and C. Neinhuis, *Planta*, 1997, **202**, 1–8.
7 S. Slagman, S. P. Pujari, M. C. R. Franssen and H. Zuilhof, *Langmuir*, 2018, **34**, 13505–13513.
8 A. Das, S. Sengupta, J. Deka, A. M. Rather, K. Raidongia and U. Manna, *J. Mater. Chem. A*, 2018, **6**, 15993–16002.
9 M. J. Liu, S. T. Wang, Z. X. Wei, Y. L. Song and L. Jiang, *Adv. Mater.*, 2009, **21**, 665–669.
10 D. Parbat and U. Manna, *Chem. Sci.*, 2017, **8**, 6092–6102.
11 L. Wang, Q. Zhou, Y. Zheng and S. Xu, *Prog. Nat. Sci.*, 2009, **19**, 1657–1664.
12 H. Hu, G. Liu and J. Wang, *J. Mater. Chem. A*, 2019, **7**, 1519–1528.
13 U. Manna and D. M. Lynn, *Adv. Mater.*, 2015, **27**, 3007–3012.
14 Y. Zhu, H. Xuan, J. Rena and L. Ge, *Soft Matter*, 2015, **11**, 8452–8459.
15 L. Barbera, L. M. D. Plano, D. Franco, G. Gattuso, S. P. P. Guglielmino, G. Lando, A. Notti, M. F. Parisi and I. Pisagatti, *Chem. Commun.*, 2018, **54**, 10203–10206.
16 Q. Wang, L. Wang, L. Gao, L. Yu, W. Feng, N. Liu, M. Xu, X. Li, P. Li and W. Huang, *J. Mater. Chem. B*, 2019, **7**, 3865–3875.
17 J. Ko, D. Kim, Y. Song, S. Lee, M. Kwon, S. Han, D. Kang, Y. Kim, J. Huh, J. S. Koh and J. Cho, *ACS Nano*, 2020, **14**, 11906–11918.
18 A. Borbora, R. L. Dupont, Y. Xu, X. Wang and U. Manna, *Mater. Horiz.*, 2022, **9**, 991–1001.
19 D. Jeon, H. Kim, C. Lee, Y. Han, M. Gu, B. S. Kim and J. Ryu, *ACS Appl. Mater. Interfaces*, 2017, **9**, 40151–40161.
20 D. G. Shchukin, M. Zheludkevich, K. Yasakau, S. Lamaka, M. G. S. Ferreira and H. Möhwald, *Adv. Mater.*, 2006, **18**, 1672–1678.
21 S. A. Hasimad, M. C. C. Romero, E. Cummins, J. P. Kerry and M. A. Morris, *J. Colloid Interface Sci.*, 2016, **461**, 239–248.

22 Z. Poon, D. Chang, X. Zhao and P. T. Hammond, *ACS Nano*, 2011, **5**, 4284–4292.
23 Z. Li and Z. Guo, *Nanoscale*, 2019, **11**, 22636–22663.
24 J. Zeng and M. Matsusaki, *Polym. Chem.*, 2019, **10**, 2960–2974.
25 D. Gaddes, H. Jung, A. P. Francesch, G. Dion, S. Tadigadapa, W. J. Dressick and M. C. Demirel, *ACS Appl. Mater. Interfaces*, 2016, **8**, 20371–20378.
26 X. Wang, Y. Wang, S. Bi, Y. Wang, X. Chen, L. Qiu and J. Sun, *Adv. Funct. Mater.*, 2014, **24**, 403–411.
27 X. Wang, F. Liu, X. Zheng and J. Sun, *Angew. Chem., Int. Ed.*, 2011, **50**, 11378–11381.
28 T. R. Cook, Y.-R. Zheng and P. J. Stang, *Chem. Rev.*, 2012, **113**, 734–777.
29 M. Zhang, D. Xu, X. Yan, J. Chen, S. Dong, B. Zheng and F. Huang, *Angew. Chem., Int. Ed.*, 2012, **124**, 7117–7121.
30 P. Cordier, F. Tournilhac, C. S. Ziakovic and L. Leibler, *Nature*, 2008, **451**, 977–980.
31 Y. Li, X. Wang and J. Sun, *Chem. Soc. Rev.*, 2012, **41**, 5998–6009.
32 R. Yuan, C. Luo, Y. Yang, C. He, Z. Lu and L. Ge, *Adv. Mater. Interfaces*, 2020, **7**, 1901873.
33 D. Xing, C.-C. Lin, Y.-L. Ho, A. Syazwan, A. Kamal, I.-T. Wang, C.-C. Chen, C.-Y. Wen, C.-W. Chen and J.-J. Delaunay, *Adv. Funct. Mater.*, 2020, **31**, 2006283.
34 J.-Y. Shiu, C.-W. Kuo, P. Chen and C.-Y. Mou, *Chem. Mater.*, 2004, **16**, 561–564.
35 J. Yong, F. Chen, Q. Yang, J. Huo and X. Hou, *Chem. Soc. Rev.*, 2017, **46**, 4168–4217.
36 S. P. Garcia, H. Bao and M. A. Hines, *Surf. Sci.*, 2003, **541**, 252–261.
37 Y. Qing, C. Hu, C. Yang, K. An, F. Tang, J. Tan and C. Liu, *ACS Appl. Mater. Interfaces*, 2017, **9**, 16571–16580.
38 J. Sun, J. Sun, Y. Li, G. Liu, F. Chu, C. Chen, Y. Zhang, H. Tian and Y. Song, *Langmuir*, 2020, **36**, 9952–9959.
39 G. Pan, J. Yin, K. Ji, X. Li, X. Cheng, H. Jin and J. Liu, *Sci. Rep.*, 2017, **7**, 6132.
40 C. Wei, G. Zhang, Q. Zhang, X. Zhan and F. Chen, *ACS Appl. Mater. Interfaces*, 2016, **8**, 34810–34819.
41 Y. Ding, W. Li, A. Correia, Y. Yang, K. Zheng, D. Liu, D. W. Schubert, A. R. Boccaccini, H. A. Santos and J. A. Roether, *ACS Appl. Mater. Interfaces*, 2018, **10**, 14540–14548.
42 A. Tombesi, S. Li, S. Sathasivam, K. Page, F. L. Heale, C. Pettinari, C. J. Carmalt and I. P. Parkin, *Sci. Rep.*, 2019, **9**, 7549.
43 E. Ozkan, C. C. Crick, A. Taylor, E. Allan and I. P. Parkin, *Chem. Sci.*, 2016, **7**, 5126–5131.
44 M. Zhang, X. Zhao, G. Zhang, G. Wei and Z. Su, *J. Mater. Chem. B*, 2017, **5**, 1699–1711.
45 V. Chernikova, O. Shekhah and M. Eddaoudi, *ACS Appl. Mater. Interfaces*, 2016, **8**, 20459–20464.
46 S. Wang, X. Zhao, Y. Tong, Q. Tang and Y. Liu, *Adv. Mater. Interfaces*, 2020, **7**, 1901950.
47 S. Ha, R. Janissen, Y. Y. Ussembayev, M. M. Oene, B. Solano and N. H. Dekker, *Nanoscale*, 2016, **8**, 10739–10748.
48 C.-G. Wang, C. Chen, K. Sakakibara, Y. Tsujii and A. Goto, *Angew. Chem., Int. Ed.*, 2018, **57**, 13504–13508.
49 E. Lee and K.-H. Lee, *Sci. Rep.*, 2018, **8**, 4101.
50 X. Zhang, H. Chen and H. Zhang, *Chem. Commun.*, 2007, 1395–1405.
51 C. L. Carpenter, S. Nicaise, P. L. Theofanis, D. Shykind, K. K. Berggren, K. T. Delaney and G. H. Fredrickson, *Macromolecules*, 2017, **50**, 8258–8266.
52 S. Liang, Y. Guan and Y. Zhang, *ACS Omega*, 2019, **4**, 5650–5660.
53 J. Shen, Y. Pei, P. Dong, J. Ji, Z. Cui, J. Yuan, R. Baines, P. M. Ajayan and M. Ye, *Nanoscale*, 2016, **8**, 9641–9647.
54 R. M. DuChanois, R. Epsztein, J. A. Trivedi and M. Elimelech, *J. Membr. Sci.*, 2019, **581**, 413–420.
55 A. P. R. Johnston, E. S. Read and F. Caruso, *Nano Lett.*, 2005, **5**, 953–956.
56 J. Wu, H. Zeng, X. Li, X. Xiang, Y. Liao, Z. Xue, Y. Ye and X. Xie, *Adv. Energy Mater.*, 2018, **8**, 1802430.
57 L. Zhang, L. Zhu, S. R. Larson, Y. Zhao and X. Wang, *Soft Matter*, 2018, **14**, 4541–4550.
58 T. B. Taketa, D. M. dos Santos, A. Fiamingo, J. M. Vaz, M. M. Beppu, S. P. Campana-Filho, R. E. Cohen and M. F. Rubner, *Langmuir*, 2018, **34**, 1429–1440.
59 Y.-N. Zhao, J. Gu, S. Jia, Y. Guan and Y. Zhang, *Soft Matter*, 2016, **12**, 1085–1092.
60 V. Selin, A. Aliakseyeu, J. F. Ankner and S. A. Sukhishvili, *Macromolecules*, 2019, **52**, 4432–4440.
61 Z. Z. Yang, X. G. Ding and J. Jiang, *Nano Res.*, 2016, **9**, 787–799.
62 M. Salomäki, J. Kauppila, J. Kankare and J. Lukkari, *Langmuir*, 2018, **34**, 13171–13182.
63 X. You, H. Wu, R. Zhang, Y. Su, L. Cao, Q. Yu, J. Yuan, K. Xiao, M. He and Z. Jiang, *Nat. Commun.*, 2019, **10**, 4160.
64 H. Fujita and T. Michinobu, *Soft Matter*, 2018, **14**, 9055–9060.
65 R. Fang, H. Zhang, L. Yang, H. Wang, Y. Tian, X. Zhang and L. Jiang, *J. Am. Chem. Soc.*, 2016, **138**, 16372–16379.
66 M. Sun, C. Zhang, J. Wang, C. Sun, Y. Ji, S. Cheng and H. Liu, *Adv. Electron. Mater.*, 2020, **6**, 2000731.
67 H. R. Alanagh, I. Rostami, M. Taleb, X. Gao, Y. Zhang, A. M. Khattak, X. He, L. Li and Z. Tang, *J. Mater. Chem. B*, 2020, **8**, 7899–7903.
68 A. G. Skirtach, A. M. Yashchenoka and H. Möhwalda, *Chem. Commun.*, 2011, **47**, 12736–12746.
69 J. E. Wong and W. Richtering, *Curr. Opin. Colloid Interface Sci.*, 2008, **13**, 403–412.
70 H. Ai, S. A. Jones and Y. M. Lvov, *Cell Biochem. Biophys.*, 2003, **39**, 23–43.
71 J. Lipton, G.-M. Weng, J. A. Röhr, H. Wang and A. D. Taylor, *Matter*, 2020, **2**, 1148–1165.
72 D. Parbat, N. Jana, M. Dhar and U. Manna, *ACS Appl. Mater. Interfaces*, 2022, DOI: **10.1021/acsami.2c04759**.
73 Q. An, T. Huang and F. Shi, *Chem. Soc. Rev.*, 2018, **47**, 5061–5098.
74 C. B. Bucur, Z. Sui and J. B. Schlenoff, *J. Am. Chem. Soc.*, 2006, **128**, 13690–13691.
75 K. Ariga, J. P. Hill and Q. Ji, *Phys. Chem. Chem. Phys.*, 2007, **9**, 2319–2340.

76 R. R. Costaab and J. F. Mano, *Chem. Soc. Rev.*, 2014, **43**, 3453–3479.
77 N. Fukao, K.-H. Kyung, K. Fujimoto and S. Shiratori, *Macromolecules*, 2011, **44**, 2964–2969.
78 F. Carosio, M. Ghanadpour, J. Alongi and L. Wågberg, *Carbohydr. Polym.*, 2018, **202**, 479–487.
79 D. J. C. Gomes, N. C. de Souza and J. R. Silva, *Measurement*, 2013, **46**, 3623–3627.
80 C. R. Crick, J. A. Gibbons and I. P. Parkin, *J. Mater. Chem. A*, 2013, **1**, 5943–5948.
81 Z. Wang, Y. Wang and G. Liu, *Angew. Chem., Int. Ed.*, 2016, **55**, 1291–1294.
82 H. Guo, M. Chen, Q. Liu, Z. Wang, S. Cui and G. Zhang, *Desalination*, 2015, **365**, 108–116.
83 J. Li, L. Li, X. Du, W. Feng, A. Welle, O. Trapp, M. Grunze, M. Hirtz and P. A. Levkin, *Nano Lett.*, 2015, **15**, 675–681.
84 H.-C. Yang, K.-J. Liao, H. Huang, Q.-Y. Wu, L.-S. Wana and Z.-K. Xu, *J. Mater. Chem. A*, 2014, **2**, 10225–10230.
85 S. Amigoni, E. T. Givenchy, M. Dufa and F. Guittard, *Langmuir*, 2009, **25**, 11073–11077.
86 D. P. Nair, M. Podgorski, S. Chatani, T. Gong,, W. Xi, C. R. Fenoli and C. N. Bowman, *Chem. Mater.*, 2014, **26**, 724–744.
87 C. F. Nising and S. Brase, *Chem. Soc. Rev.*, 2008, **37**, 1218–1228.
88 J. L. Vicario, D. Badia and L. Carrillo, *Synthesis*, 2007, 2065–2092.
89 M. E. Buck, A. S. Breitbach, S. K. Belgrade, H. E. Blackwell and D. M. Lynn, *Biomacromolecules*, 2009, **10**, 1564–1574.
90 M. E. Buck, J. Zhang and D. M. Lynn, *Adv. Mater.*, 2007, **19**, 3951–3955.
91 Y. Zhang, Y. Guan and S. Zhou, *Biomacromolecules*, 2005, **6**, 2365–2369.
92 H. Zheng, I. Lee, M. Rubner and P. Hammond, *Adv. Mater.*, 2002, **14**, 569–572.
93 J. Borges, L. C. Rodrigues, R. L. Reis and J. F. Mano, *Adv. Funct. Mater.*, 2014, **24**, 5624–5648.
94 X. Hu, E. McIntosh, M. G. Simon, C. Staii and S. W. Thomas, *Adv. Mater.*, 2016, **28**, 715–721.
95 L. Xu, H. Wang, Z. Chu, L. Cai, H. Shi, C. Zhu, D. Pan, J. Pan, X. Fei and Y. Lei, *ACS Appl. Polym. Mater.*, 2020, **2**, 741–750.
96 A. Zhuka and S. A. Sukhishvili, *Soft Matter*, 2013, **9**, 5149–5154.
97 P. Esmaeilzadeh, A. Köwitsch, A. Liedmann, M. Menzel, B. Fuhrmann, G. Schmidt, J. Klehm and T. Groth, *ACS Appl. Mater. Interfaces*, 2018, **10**, 8507–8518.
98 X.-J. Zhang, X.-W. Wang, X.-D. Da, Y. Shi, C. Liu, F. Sun, S. Yang and W.-B. Zhang, *Biomacromolecules*, 2018, **19**, 1065–1073.
99 W.-B. Zhang, F. Sun, D. A. Tirrell and F. H. Arnold, *J. Am. Chem. Soc.*, 2013, **135**, 13988–13997.
100 K. Saito and T. Miyauchi, *J. Nucl. Sci. Technol.*, 1982, **19**, 145–150.
101 J. Huang, S. Z. Moghaddam and E. Thormann, *ACS Omega*, 2019, **4**, 2019–2029.
102 L. Tauk, A. P. Schröder, G. Decher and N. Giuseppone, *Nat. Chem.*, 2009, **1**, 649–656.
103 R. F. Borch, M. D. Bernstein and H. D. Durst, *J. Am. Chem. Soc.*, 1971, **93**, 2897–2904.
104 P. Ott, K. Trenkenschuh, J. Gensel, A. Fery and A. Laschewsky, *Langmuir*, 2010, **26**, 18182–18188.
105 D. Kovacevic, S. Burgh, A. Keizer and M. A. C. Stuart, *Langmuir*, 2002, **18**, 5607–5612.
106 A. J. Nolte, N. Takane, E. Hindman, W. Gaynor, M. F. Rubner and R. E. Cohen, *Macromolecules*, 2007, **40**, 5479–5486.
107 J. J. Harris, P. M. DeRose and M. L. Bruening, *J. Am. Chem. Soc.*, 1999, **121**, 1978–1979.
108 W.-S. Jang, A. T. Jensen and J. L. Lutkenhaus, *Macromolecules*, 2010, **43**, 9473–9479.
109 J. Q. Sun, T. Wu, F. Liu, Z. Q. Wang, X. Zhang and J. C. Shen, *Langmuir*, 2000, **16**, 4620–4624.
110 I. Pastoriza-Santos, B. Scholer and F. Caruso, *Adv. Funct. Mater.*, 2001, **11**, 122–128.
111 S. Leporatti, A. Voigt, R. Mitlohner, G. Sukhorukov, E. Donath and H. Mohwald, *Langmuir*, 2000, **16**, 4059–4063.
112 X. Guo, M. C. D. Carter, V. Appadoo and D. M. Lynn, *Biomacromolecules*, 2019, **20**, 3464–3474.
113 J. F. Quinn, A. P. R. Johnston, G. K. Such, A. N. Zelikin and F. Caruso, *Chem. Soc. Rev.*, 2007, **36**, 707–718.
114 U. Manna, M. C. D. Carter and D. M. Lynn, *Adv. Mater.*, 2013, **25**, 3085–3089.
115 C. E. Hoyle, T. Y. Lee and T. Roper, *J. Polym. Sci., Part A: Polym. Chem.*, 2004, **42**, 5301–5338.
116 Y. Xin and J. Yuan, *Polym. Chem.*, 2012, **3**, 3045–3055.
117 Y. Jia and J. Li, *Chem. Rev.*, 2015, **115**, 1597–1621.
118 K.-S. Liao, A. Wan, J. D. Batteas and D. E. Bergbreiter, *Langmuir*, 2008, **24**, 4245–4253.
119 S. M. Heilmann, J. K. Rasmussen and L. R. Krepski, *J. Polym. Sci.: Part A*, 2001, **39**, 3655–3677.
120 H. Mao, A. Lin, Y. Tang, Y. Shi, H. Hu, Y. Cheng and C. Zhu, *Org. Lett.*, 2013, **15**, 4062–4065.
121 X. Su, B.-S. Kim, S. R. Kim, P. T. Hammond and D. J. Irvine, *ACS Nano*, 2009, **3**, 3719–3729.
122 L. Duan, X. Yan, A. Wang, Y. Jia and J. Li, *ACS Nano*, 2012, **6**, 6897–6904.
123 J. E. Squires, *Science*, 2002, **295**, 1002–1005.
124 S. F. Rabiner, K. O'Brien, G. W. Peskin and L. H. Friedman, *Ann. Surg.*, 1970, **171**, 615–622.
125 X.-W. Lu, W. Liu, Z.-Q. Wu, X.-H. Xiong, Q. Liu, W.-J. Zhana and H. Chen, *J. Mater. Chem. B*, 2016, **4**, 1458–1465.
126 X. Deng, N. M. Smeets, C. Sicard, J. Wang, J. D. Brennan, C. D. Filipe and T. Hoare, *J. Am. Chem. Soc.*, 2014, **136**, 12852–12855.
127 S. Chen, X. Li, Z. L. Yang, S. Zhou, R. F. Luo, M. F. Maitz, Y. C. Zhao, J. Wang, K. P. Xiong and N. Huang, *Colloids Surf., B*, 2014, **113**, 125–133.
128 Y. Xie, L. Chen, X. Zhang, S. Chen, M. Zhang, W. Zhao, S. Sun and C. Zhao, *J. Colloid Interface Sci.*, 2018, **510**, 308–317.

129 L. A. Connal, C. R. Kinnane, A. N. Zelikin and F. Caruso, *Chem. Mater.*, 2009, **21**, 576–578.
130 U. Manna, A. H. Broderick and D. M. Lynn, *Adv. Mater.*, 2012, **24**, 4291–4295.
131 M. E. Ávila-Cossío, I. A. Rivero, V. G. González, M. A. Meda, E. R. Velázquez, J. C. C. Yáñez, K. A. Espinoza and Á. P. Capiz, *ACS Omega*, 2020, **5**, 5249–5257.
132 J. Ford, S. R. Marder and S. Yang, *Chem. Mater.*, 2009, **21**, 476–483.
133 S. L. Bechler and D. M. Lynn, *Biomacromolecules*, 2012, **13**, 1523–1532.
134 D. Parbat and U. Manna, *J. Mater. Chem. A*, 2018, **6**, 22027–22036.
135 K. Katagiri, S. Yamazaki, K. Inumaru and K. Koumoto, *Polym. J.*, 2015, **47**, 190–194.
136 G. Elender, M. Kfihner and E. Sackmann, *Biosens. Bioelectron.*, 1966, **11**, 565–569.
137 B. J. Blaiszik, S. L. B. Kramer, S. C. Olugebefola, J. S. Moore, N. R. Sottos and S. R. White, *Annu. Rev. Mater. Res.*, 2010, **40**, 179–211.
138 S. H. Cho, S. R. White and P. V. Braun, *Adv. Mater.*, 2009, **21**, 645–649.
139 Y. Li, L. Li and J. Sun, *Angew. Chem.*, 2010, **122**, 6265–6269.
140 X. Cui, C. Zhang, R. P. Camilo, H. Zhang, A. Cobaj, M. D. Soucek and N. S. Zacharia, *Macromol. Mater. Eng.*, 2018, **303**, 1700596.
141 U. Manna and D. M. Lynn, *Adv. Mater.*, 2013, **25**, 5104–5108.
142 Y. Gu and N. S. Zacharia, *Adv. Funct. Mater.*, 2015, **25**, 3785–3792.
143 G. Xu, P. Liu, D. Pranantyo, K.-G. Neoh and E.-T. Kang, *ACS Sustainable Chem. Eng.*, 2018, **6**, 3916–3926.
144 S. Liu, Y. Cao, Z. Wu and H. Chen, *J. Mater. Chem. B*, 2020, **8**, 5529–5534.
145 L. Nyström, N. A. Rammahi, S. M. Häffner, A. A. Strömstedt, K. L. Browning and M. Malmsten, *Biomacromolecules*, 2018, **19**, 4691–4702.
146 J. A. Syed, S. Tang and X. Meng, *Sci. Rep.*, 2017, **7**, 4403.
147 M. Wu, N. An, Y. Li and J. Sun, *Langmuir*, 2016, **32**, 12361–12369.
148 C. Zong, M. Hu, U. Azhar, X. Chen, Y. Zhang, S. Zhang and C. Lu, *ACS Appl. Mater. Interfaces*, 2019, **11**, 25436–25444.
149 D. Parbat, S. Gaffar, A. M. Rather, A. Gupta and U. Manna, *Chem. Sci.*, 2017, **8**, 6542–6554.
150 M. C. D. Carter and D. M. Lynn, *Chem. Mater.*, 2016, **28**, 5063–5072.
151 Z. Chu, Y. Feng and S. Seeger, *Angew. Chem., Int. Ed.*, 2015, **54**, 2328–2338.
152 Y. Wu, B. Su, L. Jiang and A. J. Heeger, *Adv. Mater.*, 2013, **25**, 6526–6533.
153 L. P. Xu, J. Peng, Y. Liu, Y. Wen, X. Zhang, L. Jiang and S. Wang, *ACS Nano*, 2013, **7**, 5077–5083.
154 T. S. Wong, S. H. Kang, S. K. Y. Tang, E. J. Smythe, B. D. Hatton, A. Grinthal and J. Aizenberg, *Nature*, 2011, **477**, 443–447.
155 J. D. Smith, R. Dhiman, S. Anand, E. Reza-Garduno, R. E. Cohen, G. H. McKinley and K. K. Varanasi, *Soft Matter*, 2013, **9**, 1772–1780.
156 X. Yao, J. Ju, S. Yang, J. J. Wang and L. Jiang, *Adv. Mater.*, 2014, **26**, 1895–1900.
157 K. Manabe, K. H. Kyung and S. Shiratori, *ACS Appl. Mater. Interfaces*, 2015, **7**, 4763–4771.
158 B. Städler, A. D. Price, R. Chandrawati, L. H. Rigau, A. N. Zelikin and F. Caruso, *Nanoscale*, 2009, **1**, 68–73.
159 M.-Q. Zhao, N. Trainor, C. E. Ren, M. Torelli, B. Anasori and Y. Gogotsi, *Adv. Mater. Technol.*, 2019, **4**, 1800639.
160 Z. Zhou, Q. Song, B. Huang, S. Feng and C. Lu, *ACS Nano*, 2021, **15**, 12405–12417.
161 L. L. Mercato, M. M. Ferraro, F. Baldassarre, S. Mancarella, V. Greco, R. Rinaldi and S. Leporatti, *Adv. Colloid Interface Sci.*, 2014, **207**, 139–154.
162 W. Zhao, J.-J. Xu, C.-G. Shi and H.-Y. Chen, *Langmuir*, 2005, **21**, 9630–9634.
163 Y. Ma, Y. Zhang, B. Wu, W. Sun, Z. Li and J. Sun, *Angew. Chem.*, 2011, **123**, 6378–6381.
164 Y. Song, S. Qin, J. Gerringer and J. C. Grunlan, *Soft Matter*, 2019, **15**, 2311–2314.